NANO LETTERS

2007
Vol. 7, No. 8
2248−2251

Nucleation and Growth of GaN Nanowires on Si(111) Performed by Molecular Beam Epitaxy

Raffaella Calarco,*,† Ralph J. Meijers,† Ratan K. Debnath,† Toma Stoica,† Eli Sutter,‡ and Hans. Lüth†

Institute of Bio- and Nanosystems (IBN-1) and Center of Nanoelectronic Systems for Information Technology (CNI), Research Centre Jülich GmbH, D-52425 Jülich, Germany, and Center for Functional Nanomaterials, Brookhaven National Laboratory, Upton, New York 11973

Received March 30, 2007; Revised Manuscript Received May 25, 2007

ABSTRACT

GaN nanowires (NWs) have been grown on Si(111) substrates by plasma-assisted molecular beam epitaxy (PAMBE). The nucleation process of GaN-NWs has been investigated in terms of nucleation density and wire evolution with time for a given set of growth parameters. The wire density increases rapidly with time and then saturates. The growth period until the nucleation of new nanowires is terminated can be defined as the nucleation stage. Coalescence of closely spaced nanowires reduces the density for long deposition times. The average size of the well-nucleated NWs shows linear time dependence in the nucleation stage. High-resolution transmission electron microscopy measurements of alternating GaN and AlN layers give valuable information about the length and radial growth rates for GaN and AlN in NWs.

Semiconductor nanowires (NWs) deserve significant research attention owing to a quite unique combination of interesting structural and electronic properties as well as growth mechanism. In this respect, it is worth noting that nanowires can be fabricated on a wide variety of substrates, including silicon, which makes them possible candidates for future CMOS integration. An additional advantage of NW heteroepitaxy is that the nanowires can elastically relax laterally, therefore, it is possible to realize combinations of materials accommodating lattice mismatch through pseudomorphic growth without dislocation formation.

In recent years, III-nitride-based nanowires have been investigated as potential nanoelectronic devices.[1−5] GaN NWs with extremely good crystal quality and strong luminescence efficiency[6−9] have already been grown by molecular beam epitaxy (MBE) on different substrates. Studies of plasma-assisted MBE grown GaN nanowires[6] demonstrate the possibility of tuning the structural properties of nanowires, reaching tapering effect control and improvement of the crystalline quality of the nanowires. While the nanowire growth by MBE has already been established, a lot of uncertainty remains on the mechanisms driving the growth and in particular the nucleation.

The growth mechanism of GaN NWs by MBE has been subject of only very few investigations.[10−12] In our previous work,[10] we explain the growth by making use of the diffusion-induced (D-I) mechanism. The adatoms diffuse to the wire apex from its lateral sides driven by a lower chemical potential at the top surface. This D-I mechanism is used to explain the observed dependence of the wire length on the diameter for deposition times longer than the nucleation time, but a complete understanding of the growth process requires considering the nucleation stage as well.

An important difference in the MBE growth of GaN NWs compared to NW growth of most of the other III−V semiconductors is that we do not use a foreign catalyst. The catalyst enhances the growth locally and defines the position and diameter of nanowires.[13] However, this catalyst can introduce unwanted contamination in devices. The presence of a Au catalyst for instance can be detrimental to device performance in Si-based circuits. Therefore, a catalyst-free approach to grow nanowires is very interesting from the technological point of view.[14] In this case, however, control of position and diameter does not arise from catalyst position and size. Thus insights into nucleation and growth mechanisms driving the catalyst-free growth of nanowires are essential to achieve the desired control.

In the experiments, GaN NWs have been grown by radio-frequency plasma-assisted MBE on Si(111) in N-rich conditions. The set of samples discussed in this study has been grown at a substrate temperature of $T_{subs} = 785$ °C, a

* Corresponding author. E-mail: r.calarco@fz-juelich.de. Telephone: +49 (0) 2461 61 2164. Fax: +49 (0) 2461 61 2940.

† Institute of Bio- and Nanosystems (IBN-1) and Center of Nanoelectronic Systems for Information Technology (CNI), Research Centre Jülich GmbH.

‡ Center for Functional Nanomaterials, Brookhaven National Laboratory.

10.1021/nl0707398 CCC: $37.00
Published on Web 06/29/2007

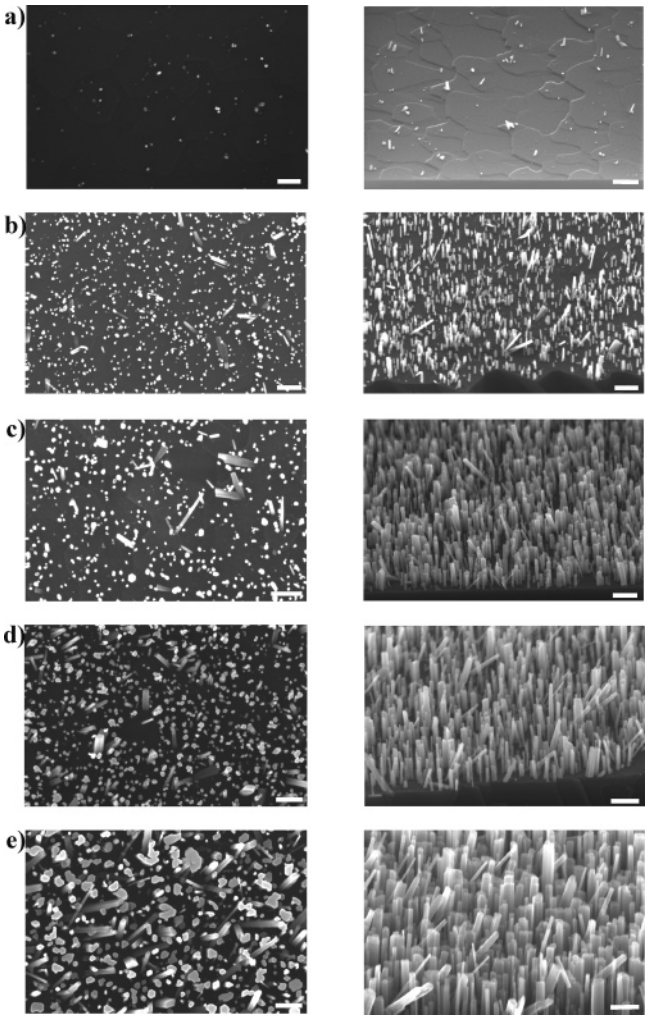

Figure 1. SEM top view (left side) and lateral-side view (right side) of GaN nanowires grown at different deposition times: (a) 15 min, (b) 30 min, (c) 45 min, (d) 60 min, (e) 90 min. The scale bars correspond to 200 nm.

Ga-beam equivalent pressure of 3.0×10^{-8} mbar, a N_2 flux of 4.0 sccm, and a forward power of 500 W of the radio-frequency plasma cell. A detailed description of the experimental growth conditions and the influence of the different parameters can be found elsewhere.[6] After the growth, the samples were investigated by scanning electron microscopy (SEM) as well as by high-resolution transmission electron microscopy (HRTEM) with respect to their morphology and crystalline quality (field-emission JEOL JEM 3000F).

The SEM images in Figure 1 show the top and side view of five different samples grown for 15, 30, 45, 60, and 90 min for parts a−e of Figure 1, respectively. From Figure 1a, it is clear that the NWs grow on the flat terraces of the Si(111) surface without any preferential nucleation sites. Sometimes at the base of the wire, a small pedestal is visible. While most of the NWs are vertically aligned with the GaN[0001]//Si[111] direction, some are tilted (angles of about 35° were observed). After 15 min of growth (Figure 1a), the density of nanowires is low and of the order of 7×10^8 NWs/cm^2 (cf. Figure 2). For a doubled deposition time (30 min), the nanowire density already increases to a value above 10^{10} NWs/cm^2, which is almost the maximum observed NW density (Figure 2). After 60 min of deposition (Figure 1d), the NW density has saturated and therefore we assume the nucleation stage to be completed. For longer deposition times, the NW density decreases due to coalescence of closely spaced NWs as a result of lateral growth of the NWs. Widely spaced wires, however, continue to grow separately. The coalescence can be seen in Figure 1e in top-view.

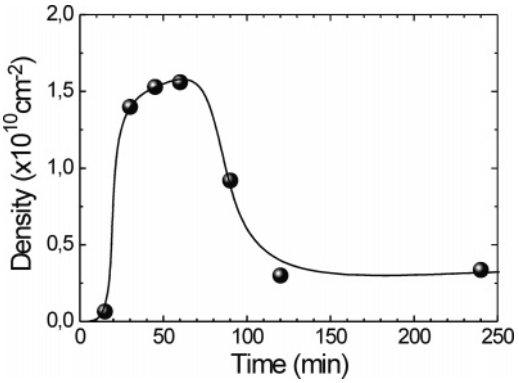

Figure 2. GaN NW density plotted as a function of deposition time (line guides the eye).

In Figure 2, the nanowire density is plotted as a function of time, and it shows the rapid increase with growth time between 15 and 60 min. As already discussed, for a growth time longer than 60 min, coalescence leads to a decrease of the nanowire density down to a value of about 3×10^9 NWs/cm^2 for deposition time longer than 120 min.

With the help of SEM images, we also measured the length or height L of the nanowires, determined as the average value of the longest NWs. Only well-developed wires were taken into account so that the measured values account for wires that have the maximum length between those present in SEM images. The length plotted as a function of deposition time is shown in Figure 3a. The observed linear time dependence of the length is similar to that reported for MBE-grown Si nanowires.[15] The diameter of these wires has been measured as well, and the average value is shown as function of deposition time (for different times up to 90 min) in Figure 3b. In Figure 3c, the volume, calculated as a mean value for the same set of wires of Figures 3a,b, is plotted as function of growth time.

Linear fit of Figure 3b for the evaluation of the most probable value of the nucleation diameter in the early stage of nucleation gives a value of about 15 nm, in agreement with the value we already reported previously.[10] This value can be assumed as an estimation of the nucleation diameter, as the accuracy for its determination is related to SEM resolution. Further and more detailed investigations using more sensitive techniques are necessary to determine it carefully. The growth rates of length and diameter evaluated from the slop of the linear fits in parts a and b of Figure 3 are about 3.2 and 0.4 nm/min, respectively. These average values will be compared later on with the results of HRTEM on single NW. The time evolution of the average volume of the NWs is a direct consequence of the length and diameter

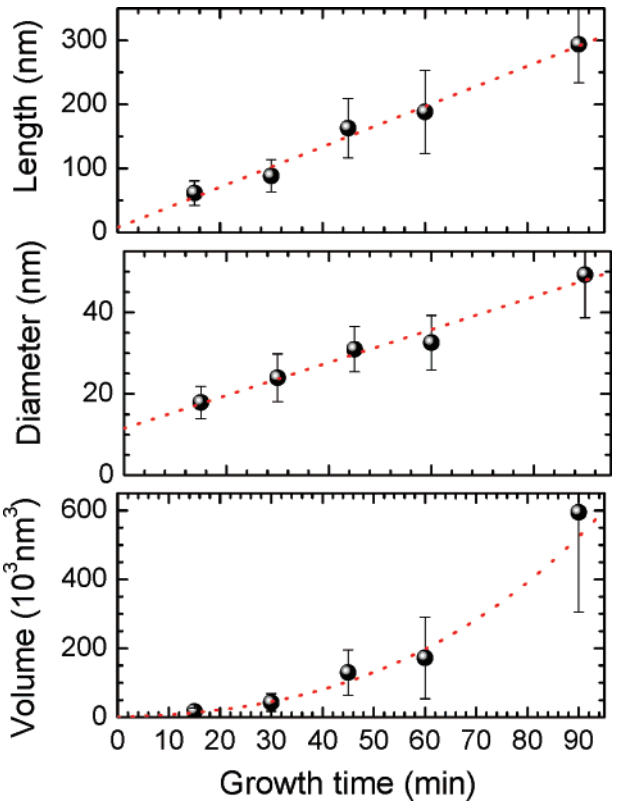

Figure 3. (a) GaN NW length distribution as a function of deposition time; (b) GaN NW diameter distribution as a function of deposition time; (c) GaN NW volume distribution as a function of deposition time. The error bars are given by standard deviation. The statistics was performed on about 40 wires per sample.

time dependence. The linear dependences found in Figure 3a,b have been used to compute the dotted curve in Figure 3c, assuming a cylindrical shape of the NWs. The curve fits well with the experimental data. We would like to note that the substrate temperature is playing an important role in the nucleation process because, at higher growth temperature (results not shown here), a longer nucleation stage was observed. Therefore, it has to be stressed again that all our studies have been performed for samples grown at the same substrate temperature (785 °C).

In addition to the dependence of the wire length on its diameter $L(d) \sim 1/d + C$ previously published,[10] the observed constant growth rate dL/dt as a function of time limits the possible atomistic transport and incorporation mechanisms contributing to the growth. The situation is similar to the growth of Si NWs by MBE in ref 15 except for the constant C. The $1/d$ behavior is best followed for longer deposition times due to the specific nucleation time of each NW, which leads to different growth times and a (statistical) distribution of NW lengths for similar diameter. Because the nucleation finishes after approximately 60 min, this effect will fade away for longer deposition times, and the intrinsic length−diameter correlation will start to dominate as shown in ref 10.

For the Si NWs,[15] the constant growth rate with time and the inverse dependence on the wire diameter leads to the following expression for the total flux incorporated into the wire:

$$\pi R^2 \, dL/dt = \gamma R \tag{1}$$

where R is the wire radius, and dL/dt is the vertical growth rate. This equation is satisfied for the case of a very fast diffusion of adatoms on the substrate and wire surface, where the flux is limited by the incorporation rate at the boundary of the whisker and the liquid droplet.

As mentioned above, we have observed the following behavior: $L(d) \sim 1/d + C$. The extra constant C can be explained if we consider an additional term $\sim R^2$ in eq 1. This corresponds to the contribution by direct impingement, which is time independent and should be proportional to πR^2. We then get the following relation:

$$\pi R^2 \, dL/dt = \gamma_T R^2 + \gamma_S R \tag{2}$$

where dL/dt is the axial or vertical growth rate and γ_T and γ_S are time-independent constants related to different contributions to the growth. Impinging atoms on the top of the wire (γ_T) and atoms diffusing from the substrate to the top (γ_S) are both taken into account in the right-hand side of eq 2. For ease of notation, the π will be suppressed in the following, which is just a redefinition of the constants γ. If we then suppose a nucleation time t_0, the solution to eq 2 is:

$$L = (\gamma_S/R + \gamma_T)(t - t_0) \tag{3}$$

which describes both the linear time dependence of the wire length as well as the dependence of the length on the reciprocal diameter.

Formula 3 is true only if the radius is constant in time. If we suppose a simple linear dependence:

$$R = R_0 + \gamma_R(t - t_0) \tag{4}$$

where γ_R is a time-independent constant. Then the solution of eq 2 is:

$$L = \gamma_T(t - t_0) + (\gamma_S/\gamma_R) \ln(R/R_0) \tag{5}$$

which is reduced to solution (eq 3) for:

$$\gamma_R(t - t_0)/R_0 \gg 1 \tag{6}$$

From the analysis of Figure 3b, an increase of the diameter with time is found, as can be also easily verified by looking at the images in Figure 1; this implies a lateral growth of the wires.

To investigate the lateral growth and compare it directly with the vertical one, a sample was prepared that contains several AlN layers. They act as time markers for post-growth analysis with HRTEM (Figure 4a). The sample consists of the following alternating GaN and AlN layers: GaN(t_{dep} = 5 min)/AlN(t_{dep} = 3 min)/2x{GaN(t_{dep} = 1 min)/2xAlN(t_{dep} = 1 min)}/2x{GaN(t_{dep} = 1 min)/AlN(t_{dep} = 30 s)}/GaN-(t_{dep} = 6 h)/ Si(111), schematically shown in Figure 4b.

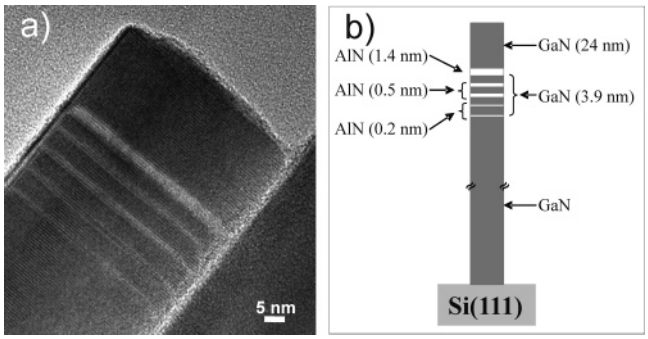

Figure 4. (a) High-magnification TEM of a NW GaN/AlN heterostructure sample; (b) growth schema of the alternating layers in the NW.

The heterostructure profile is very sharp with well-defined contrast between the GaN and AlN layers owing to the different mass contrast between Ga and Al. This is also a strong indication that the MBE growth of III-nitride NWs is not driven by a self-catalytic liquid droplet, which could smear out the interface due to a memory effect. The HRTEM image shows that GaN/AlN layer sequence is present not only at the front growth surface but also on the lateral sides of the NW indicating small but quantifiable lateral growth. From the measured thicknesses and known deposition times, a vertical growth rate of 5 nm/min for GaN and of 0.4 nm/min for AlN is evaluated. The lateral growth rates amount to 0.15 nm/min and 0.10 nm/min for GaN and AlN, respectively. Thus the ratio between the vertical and lateral growth rate is much higher for GaN than for AlN (∼33:1 vs 4:1). As discussed above, the vertical growth rate depends on diameter.[10] The lateral growth rate might also depend on wire diameter, which will be investigated in more detail in a forthcoming publication. It is worth also to mention that the growth rates obtained by these TEM investigations of a single heterostructured NW are close to the values found by SEM studies of the time evolution of NW sizes presented within the first part of the paper (Figure 3a,b).

In conclusion, experimental results on GaN NWs have been provided in order to explain the nucleation and wire growth processes. For a catalyst-free method, a relatively long nucleation stage in which new NWs appear was observed. This depends strongly on deposition parameters. For the specific growth conditions investigated in this paper, the nanowire density shows a rapid increase from 15 to 60 min of deposition. After 60 min, due to the coalescence effect, the nanowire density decreases again to a value of about 3×10^9 NWs/cm^2. During the nucleation stage, a linear dependence of the mean values of the length and the diameter on time has been found. An inverse dependence of the NW length on its diameter has been previously reported. The coexistence of both dependences is in agreement with a diffusion-induced growth mechanism. HRTEM measurements demonstrate lateral growth for GaN and AlN layers, which is much more pronounced in the latter case. In fact, the lateral growth rates amount to 3% and 25% with respect to the vertical growth for GaN and AlN, respectively. The lateral growth effect has also been taken into account in the discussed model.

Acknowledgment. We gratefully acknowledge fruitful discussions and suggestions by D. Grützmacher. We also thank K. H. Deussen for technical support. One of the authors (R.K.D.) appreciates the financial support from a Helmholtz-DAAD Fellowship. This work was performed in part under the auspices of the U.S. Department of Energy under contract no. DE-AC02-98CH1-886.

References

(1) Greytak, A.; Lauhon, L.; Gudiksen, M.; Lieber, C. M. *Appl. Phys. Lett.* **2004**, *84*, 4176.
(2) Gradečak, S.; Qian, F.; Li, Y.; Park, H.-G.; Lieber, C. M. *Appl. Phys. Lett.* **2005**, *87*, 173111.
(3) Huang, Y.; Duan, X.; Cui, Y.; Lauhon, L. J.; Kim, K.-H.; Lieber, C. M. *Science* **2001**, *294*, 9, 1313.
(4) Calarco, R.; Marso, M.; Richter, T.; Aykanat, A. I.; Meijers, R.; v.d. Hart, A.; Stoica, T.; Lüth, H. *Nano Lett.* **2005**, *5*, 981.
(5) Cavallini, A.; Polenta, L.; Rossi, M.; Richter, T.; Marso, M.; Meijers, R.; Calarco, R.; Luth, H., *Nano Lett.* **2006**, *6*, 1548.
(6) Meijers, R.; Richter, T.; Calarco, R.; Stoica, T.; Bochem, H.-P.; Marso, M.; Lüth, H. *J. Cryst. Growth* **2006**, *289*, 381.
(7) Thillosen, N.; Sebald, K.; Hardtdegen, H.; Meijers, R.; Calarco, R.; Montanari, S.; Kaluza, N.; Gutowski, J.; Lüth, H. *Nano Lett.* **2006**, *6*, 704.
(8) Calleja, E.; Sánchez-García, M. A.; Sánchez, F. J.; Calle, F.; Naranjo, F. B.; Muñoz, E.; Jahn, U.; Ploog, K. *Phys. Rev. B* **2000**, *62*, 16826.
(9) Sanchez-Paramo, J.; Calleja, J.; Sanchez-Garcia, M.; Calleja, E.; Jahn, U. *Physica E* **2002**, *13*, 1070.
(10) Debnath, R. K.; Meijers, R.; Richter, T.; Stoica, T.; Calarco, R.; Lüth, H. *Appl. Phys. Lett.* **2007**, *90*, 123117.
(11) Mamutin, V. *Tech. Phys. Lett.* **1999**, *25*, 741.
(12) Bertness, K. A.; Roshko, A.; Sanford, N. A.; Barker, J. M.; Davydov, A. V. *J. Cryst. Growth* **2006**, *287*, 522.
(13) Jensen, L.; Bjoerk, M.; Jeppesen, S.; Persson, A.; Ohlsson, B.; Samuelson, L. *Nano Lett.* **2004**, *4*, 1961.
(14) Mandl, B.; Stangl, J.; Martensson, T.; Mikkelsen, A.; Eriksson, J.; Karlsson, L.; Bauer, G.; Samuelson, L.; Seifert, W. *Nano Lett.* **2006**, *6*, 1817.
(15) Schubert, L.; Werner, P.; Zakharov, N. D.; Gerth, G.; Kolb, F. M.; Long, L.; Goesele, U. *Appl. Phys. Lett.* **2004**, *84*, 4968.

NL0707398